여기부와의 전자파 결합 현상을 고려한 위스퍼링 갤러리 모드 유전체 공진기의 공진주파수에 관한 연구

A Study on Resonance Frequencies of a Whispering Gallery Mode Dielectric Resonator Considering Electromagnetic Coupling Phenomena with an Excitation Part

황재효 · 민경일 · 구경완

Jae-Hyo Hwang · Kyoung-Il Min · Kyung-Wan Koo

요 약

위스퍼링 갤러리 모드가 동작하는 유전체 원판 공진기의 공진 특성은 모드를 여기시키기 위하여 원판 공진기 주위에 배치한 외부 회로에 의하여 영향을 받게 된다. 이러한 현상을 해석하기 위하여, 원판 공진기를 모드 결합이 일어나는 결합부와 결합이 일어나지 않는 비결합부로 나누어 해석하였다. 결합부에서는 원판을 정합회로로 임피던스 매칭한 후, 비평형 유전체 도파로의 결합 전송 방정식을 유도하였다. 결합 전송 방정식으로부터 결합 계수, 결합 전자계 분포, 전력의 이동량 및 모드 결합 현상을 고려한 공진 주파수를 계산하였다. 또한, 공진 특성에 관한 실험을 통하여, 공진 주파수의 계산치와 실험치 간의 오차가 약 1.28%이고 FSR의 경우 약 0.6%임을 알 수 있었다.

Abstract

Resonant characteristic of Whispering Gallery modes(W. G. mode) on a dielectric disk resonator is influenced by an external circuit that is placed near the disk to excite this type of modes. In order to evaluate this phenomenon, we divide the disk resonator as two parts; a coupling part in which the mode coupling occurs and an uncoupled region. In the coupled part, we regard the part of the disk as a curved waveguide which is loaded with matched circuit, and derive a coupled mode equation for nonparallel dielectric waveguides. From the coupled mode equation, we calculate coupling coefficients and a coupled electromagnetic field. By using the complex coupling coefficients, we can calculate power transfer. We also calculate a resonant frequency in consideration of the mode coupling phenomenon. The calculated resonance frequence is confirmed by experiment for the resonance characteristics. As the results, it is found that the discrepancy between the theoretical and the experimental resonance frequencies is about 1.28% and the discrepancy between theory and experiment of FSR is about 0.6%.

「본 논문은 정보통신부 산하 정보통신연구관리단 주관의 대학기초연구지원사업의 연구비를 지원받아 행하여졌음.」

영동대학교 전자공학부(Faculty of Electronics Engineering, Youngdong University)

· 논 문 번 호 : 980326-036

· 수정완료일자 : 1998년 8월 21일

I. Introduction

Dielectric circuit components are expected to play an important role for millimeter through optical wave integrated circuit. A dielectric disk resonator that operates in a Whispering Gallery (W. G.) mode will be very useful as a frequency selective device. The W. G. mode resonator has, in general, a large radius of curvature compared with an employed wavelength, and an electromagnetic field of the W. G. mode concentrates near an edge of the disk [1],[2]. Therefore, the disk (that supports the W. G. mode) can be assumed as a sort of a curved waveguide.

Several studies on the disk resonator which is isolated in a space has been reported[2],[3]. In these cases, no influence by external circuits is regarded. In practical integrated circuits, the disk resonator is located beside an external circuit that excites the W. G. mode on the disk and picks up the resonance response. In this case, an electromagnetic mode of the external circuit has an influence on a resonance characteristics of the W. G. mode. The influence on the resonance characteristics is caused by mode coupling between the two modes that are the W. G. mode of the disk and the propagating mode of external circuit. The mode coupling phenomenon occurs only inside a region where a part of the disk approaches the external circuit. We call the region as a coupled region. For calculation of the resonance characteristics of the W. G. mode precisely, it is necessary to analyze the effect of the mode coupling on the coupled region in detail.

In this paper, we calculate resonance frequencies of the W. G. mode on the dielectric disk resonator excited by an external dielectric rectangular waveguide, considering the influence of the mode coupling. We suppose that the disk resonator with the external waveguide consists two regions, i.e. a coupled region and an uncoupled region.

In the coupled region, the W. G. mode in the disk couples to the propagating mode in the external waveguide. Since we can regard the disk in this region as a curved dielectric waveguide, we solve a coupled mode problem for nonparallel and curved dielectric waveguides to know the coupling characteristics. We show here a general way to derive a coupled mode equation for the nonparallel and curved dielectric waveguides, and apply this method to the coupled region. We introduce a global coordinate system to express an entire coupled field and solve the coupled mode equation numerically. As a result, we show numerical results of the coupling characteristics such as coupling coefficients, coupled mode field and power transfer on the coupled region. Finally, we obtain a scattering parameter(S-parameter) matrix for this coupled region by calculating modal amplitudes.

In the uncoupled region, the W. G. mode propagates without any influence of the coupling phenomenon. So, we can obtain a S-parameter matrix for the uncoupled region from the modal amplitudes of the W. G. mode on the disk which is calculated in a conventional analysis for an isolated disk resonator[3].

From these S-matrix equations for the coupled region and the uncoupled region, we can obtain a S-matrix equation for the disk resonator with the external waveguide. Solving the S-matrix equation at various frequencies, we can find the resonance frequencies for the resonator system.

Ⅱ. Coupled mode equation for nonparallel and curved waveguides

A coupled structure that consists of two curved dielectric waveguides is shown in Fig. 1.

Two local orthogonal coordinate systems (x', y', z') and (x'', y'', z'') are also shown in the figure and are combined to a global coordinate system (x, y, z). We suppose that an electromagnetic field and a relative dielectric constant of the coupled structure are expressed by $\{\boldsymbol{E}_c(x, y, z), \boldsymbol{H}_c(x, y, z)\}$ and $\varepsilon_c(x, y, z)$, respectively. The electromagnetic field can be expressed approximately as a sum of two electromagnetic fields with weighting functions $m_1(z)$ and $m_2(z)$ as shown in Eq. 1. One is an electromagnetic field $\{\boldsymbol{E}_1(x', y', z'), \boldsymbol{H}_1(x', y', z')\}$ which is an intrinsic mode of the isolated curved dielectric waveguide #1 and the another is an electromagnetic field $\{\boldsymbol{E}_2(x'', y'', z''), \boldsymbol{H}_2(x'', y'', z'')\}$ which is an intrinsic mode of the isolated curved dielectric waveguide # 2 as shown in Fig. 2(a) and (b).

In the above equations, the symbol ^ denotes an unit vector and the subscripts t and z denote transverse and longitudinal components, respectively. This expression is reasonable to

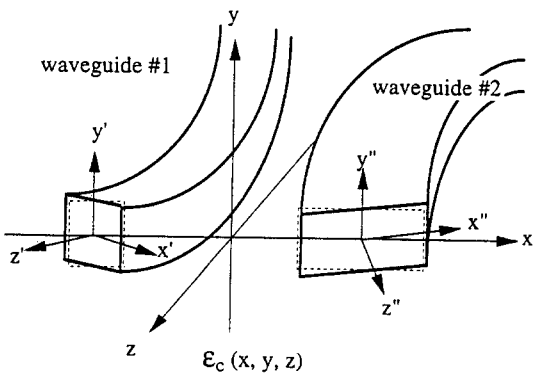

Fig. 1. Coupled structure of two nonparallel and curved waveguides.

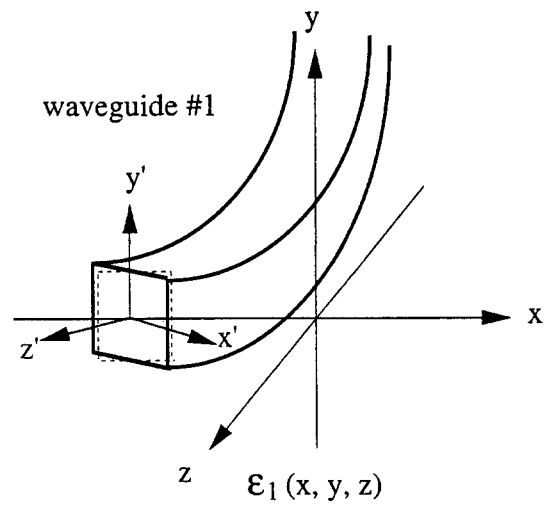

Fig. 2. (a) The isolated curved dielectric waveguide #1

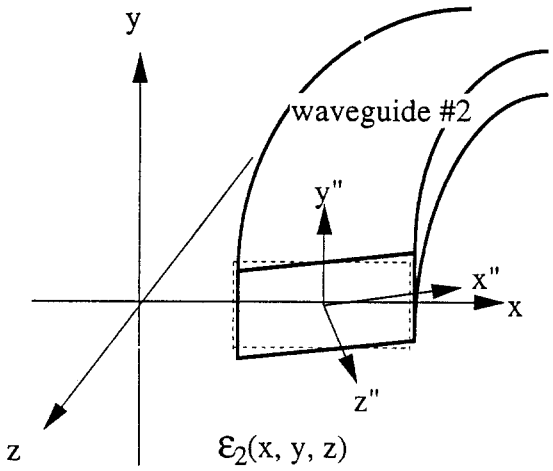

Fig. 2. (b) The isolated curved idelectric waveguide #2

$$\boldsymbol{E}_c(x,y,z)=m_1(z)\exp[-j\gamma_1(x,y,z)](\boldsymbol{E}_{1t}+\frac{\varepsilon_1}{\varepsilon_c}E_{1z}\hat{z})$$
$$+m_2(z)\exp[-j\gamma_2(x,y,z)](\boldsymbol{E}_{2t}+\frac{\varepsilon_2}{\varepsilon_c}E_{2z}\hat{z})$$
$$\boldsymbol{H}_c(x,y,z)=m_1(z)\exp[-j\gamma_1(x,y,z)](\boldsymbol{H}_{1t}+H_{1z}\hat{z})$$
$$+m_2(z)\exp[-j\gamma_2(x,y,z)(\boldsymbol{H}_{2t}+H_{2z}\hat{z}) \quad (1)$$

the case that a difference of the dielectric

constants between guides and surrounding medium is not so large[4].

In the following analysis, we express briefly the propagating factors of the electromagnetic mode $\gamma_1(x, y, z)$ and $\gamma_2(x, y, z)$ as γ_1 and γ_2. They have a dimension of radian. If we know the weighting functions $m_1(z)$ and $m_2(z)$, we can obtain the coupling characteristics of the electromagnetic field. In order to know the weighting functions, we derive two sets of equations on the weighting functions. We apply the Lorentz reciprocity theorem[5] and divergence theorem to the two sets of field combination ($\{\boldsymbol{E}_c, \boldsymbol{H}_c\}$, $\{\boldsymbol{E}_1, \boldsymbol{H}_1\}$) and ($\{\boldsymbol{E}_c, \boldsymbol{H}_c\}$, $\{\boldsymbol{E}_2, \boldsymbol{H}_2\}$), then we obtain the following two equations;

$$\hat{z}\cdot\frac{\partial}{\partial z}\iint_{-\infty}^{\infty}(\boldsymbol{E}_c\times\boldsymbol{H}_l-\boldsymbol{E}_l\times\boldsymbol{H}_c)dxdy$$
$$=j\omega\varepsilon_0\iint_{-\infty}^{\infty}(\varepsilon_c-\varepsilon_l)\boldsymbol{E}_c\cdot\boldsymbol{E}_l\,dxdy$$
where $l=1, 2$. (2)

By substituting the Eq. 1 into the Eq. 2, we can derive a set of simultaneous differential equation for weighting functions $m_1(z)$ and $m_2(z)$ as follows;

$$\frac{\partial}{\partial z}\left[m_1(z)\iint_{-\infty}^{\infty}\frac{e^{-j(\gamma_1-\gamma_2)}}{\omega\varepsilon_0}(\boldsymbol{E}_{1t}\times\boldsymbol{H}_{2t}+\boldsymbol{E}_{2t}\times\boldsymbol{H}_{1t})\cdot\hat{z}\,dxdy\right]$$
$$+\frac{\partial}{\partial z}\left[m_2(z)\iint_{-\infty}^{\infty}\frac{2}{\omega\varepsilon_0}(\boldsymbol{E}_{2t}\times\boldsymbol{H}_{2t})\cdot\hat{z}\,dxdy\right]$$
$$=-m_1(z)\iint_{-\infty}^{\infty}(\varepsilon_c-\varepsilon_2)\,e^{-j(\gamma_1-\gamma_2)}(\boldsymbol{E}_{1t}\cdot\boldsymbol{E}_{2t}-\frac{\varepsilon_1}{\varepsilon_c}E_{1z}E_{2t})dxdy$$
$$-m_2(z)\iint_{-\infty}^{\infty}(\varepsilon_c-\varepsilon_2)(\boldsymbol{E}_{2t}\cdot\boldsymbol{E}_{2t}-\frac{\varepsilon_2}{\varepsilon_c}E_{2z}^2)dxdy \quad (3a)$$

and

$$\frac{\partial}{\partial z}\left[m_1(z)\iint_{-\infty}^{\infty}\frac{2}{\omega\varepsilon_0}(\boldsymbol{E}_{1t}\times\boldsymbol{H}_{1t})\cdot\hat{z}\,dxdy\right]$$
$$+\frac{\partial}{\partial z}\left[m_2(z)\iint_{-\infty}^{\infty}\frac{e^{-j(\gamma_2-\gamma_1)}}{\omega\varepsilon_0}(\boldsymbol{E}_{2t}\times\boldsymbol{H}_{1t}+\boldsymbol{E}_{1t}\times\boldsymbol{H}_{2t})\cdot\hat{z}\,dxdy\right]$$
$$=-m_1(z)\iint_{-\infty}^{\infty}(\varepsilon_c-\varepsilon_1)(\boldsymbol{E}_{1t}\cdot\boldsymbol{E}_{1t}-\frac{\varepsilon_1}{\varepsilon_c}E_{1z}^2)dxdy$$
$$=-m_2(z)\iint_{-\infty}^{\infty}(\varepsilon_c-\varepsilon_1)\,e^{-j(\gamma_2-\gamma_1)}(\boldsymbol{E}_{2t}\cdot\boldsymbol{E}_{1t}-\frac{\varepsilon_1}{\varepsilon_c}E_{2z}E_{1z})dxdy \quad (3b)$$

We can rewrite above equations into the following simple form,

$$\frac{\partial[F_1m_1(z)]}{\partial z}+\frac{\partial[F_2m_2(z)]}{\partial z}=-jm_1(z)F_3-jm_2(z)F_4$$
$$\frac{\partial[F_5m_1(z)]}{\partial z}+\frac{\partial[F_6m_2(z)]}{\partial z}=-jm_1(z)F_7-jm_2(z)F_8 \quad (4)$$

where,

$$F_1=\iint_{-\infty}^{\infty}\frac{\exp[-j(\gamma_1-\gamma_2)]}{\omega\varepsilon_0}(\boldsymbol{E}_{1t}\times\boldsymbol{H}_{2t}+\boldsymbol{E}_{2t}\times\boldsymbol{H}_{1t})\cdot\hat{z}\,dxdy$$
$$F_2=\iint_{-\infty}^{\infty}\frac{2}{\omega\varepsilon_0}(\boldsymbol{E}_{2t}\times\boldsymbol{H}_{2t})\cdot\hat{z}\,dxdy$$
$$F_3=\iint_{-\infty}^{\infty}(\varepsilon_c-\varepsilon_2)\exp[-j(\gamma_1-\gamma_2)](\boldsymbol{E}_{1t}\cdot\boldsymbol{E}_{2t}-\frac{\varepsilon_1}{\varepsilon_0}E_{1z}E_{2z})dxdy$$
$$F_4=\iint_{-\infty}^{\infty}(\varepsilon_c-\varepsilon_2)(\boldsymbol{E}_{1t}\cdot\boldsymbol{E}_{2t}-\frac{\varepsilon_1}{\varepsilon_c}E_{2z}^2)dxdy$$
$$F_5=\iint_{-\infty}^{\infty}\frac{2}{\omega\varepsilon_0}(\boldsymbol{E}_{1t}\times\boldsymbol{H}_{1t})\cdot\hat{z}\,dxdy$$
$$F_6=\iint_{-\infty}^{\infty}\frac{\exp[-j(\gamma_2-\gamma_1)]}{\omega\varepsilon_0}(\boldsymbol{E}_{2t}\times\boldsymbol{H}_{1t}+\boldsymbol{E}_{2t}\times\boldsymbol{H}_{2t})\cdot\hat{z}\,dxdy$$
$$F_7=\iint_{-\infty}^{\infty}(\varepsilon_c-\varepsilon_1)(\boldsymbol{E}_{1t}\cdot\boldsymbol{E}_{1t}-\frac{\varepsilon_1}{\varepsilon_c}E_{1z}^2)dxdy$$
$$F_8=\iint_{-\infty}^{\infty}(\varepsilon_c-\varepsilon_1)\exp[-j(\gamma_2-\gamma_1)](\boldsymbol{E}_{2t}\cdot\boldsymbol{E}_{1t}-\frac{\varepsilon_1}{\varepsilon_c}E_{2z}E_{1z})dxdy \quad (5)$$

From Eq. 4, we can derive a simultaneous equation for $m_1(z)$ and $m_2(z)$ in a matrix form as follows;

$$\begin{bmatrix} \frac{\partial m_1(z)}{\partial z} \\ \frac{\partial m_2(z)}{\partial z} \end{bmatrix} = \begin{bmatrix} K_{11}(z) & K_{12}(z) \\ K_{21}(z) & K_{22}(z) \end{bmatrix} \begin{bmatrix} m_1(z) \\ m_2(z) \end{bmatrix} \quad (6)$$

where,

$$K_{11}(z)=\frac{1}{F_1F_6-F_2F_5}[F_2(jF_7+\frac{\partial F_5}{\partial z})-F_6(jF_3+\frac{\partial F_1}{\partial z})]$$

$$K_{12}(z)=\frac{1}{F_1F_6-F_2F_5}[F_2(jF_8+\frac{\partial F_6}{\partial z})-F_6(jF_4+\frac{\partial F_2}{\partial z})]$$

$$K_{21}(z)=\frac{1}{F_1F_6-F_2F_5}[F_5(jF_3+\frac{\partial F_1}{\partial z})-F_1(jF_7+\frac{\partial F_5}{\partial z})]$$

$$K_{22}(z)=\frac{1}{F_1F_6-F_2F_5}[F_5(jF_4+\frac{\partial F_2}{\partial z})-F_1(jF_8+\frac{\partial F_6}{\partial z})] \quad (7)$$

The functions $m_1(z)$ and $m_2(z)$ can be obtained by solving Eq. 6 numerically with actual dimensions of the curved dielectric waveguides system.

Ⅲ. Numerical calculation

The W. G. mode in a dielectric disk is regarded as a propagating mode in a curved dielectric waveguide. The coupled mode equation in chapter 2 can be applied to the coupled region of Fig. 3.

In this analysis, we assume that only the $WGH_{m,1,1}$ propagates in the disk and the mode coupling occurs only in the coupled region; no mode coupling occurs on outside of this region. In order to solve the coupled mode equation, we calculate coupling coefficients $K_{mm}(z)$ in Eq. 6 that are obtained by calculating the double integrals of intrinsic modes in Eq. 3. In the calculation, we choose the following parameters to obtain the coupling coefficients. The complex dielectric constants of the disk and the straight waveguide (ε_r) are $2.06 - j\,5.86\times10^{-4}$ and a dielectric constant of a surrounding media (ε_1) is 1.0. Frequency (f) is 24 GHz or the wavelength (λ) is 1.25×10^{-2} m. Dimensions of the disk and the straight waveguide are as follows; a radius of curvature of the disk R is 8λ, a thickness of the disk (H) is 0.64λ and a cross section of the straight waveguide is 0.64λ 0.64λ. The propagation constant of the W. G. mode in the disk [$\gamma_1/(R\theta)$] is 581.45 $-j$ 0.129 (m^{-1})[6] and that of the fundamental mode in the straight waveguide (γ_2/z) is 590.81 $-j$ 0.135 (m^{-1}). A minimum distance between the disk and the straight waveguide (d) is zero. Fig. 4 shows the calculated coupling coefficients between the W. G. mode of the disk and the propagating mode of the straight waveguide.

The coupling coefficients $K_{mn}(z)$(where m, n=1 or 2) presents coupling rate of transmitting power from waveguide #n to waveguide #m. In this figure, we find that the mode coupling occurs distinctly in a range of -60 mm

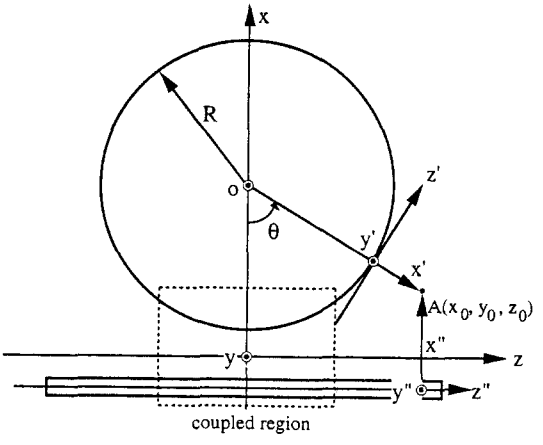

Fig. 3. The coupled region of a part of the disk resonator and the straight waveguide. θ is a relation angle between the global coordinate (x, y, z) and a local coordinates (x', y', z'). A coordinate system (x'', y'', z'') is an another local coordinate.

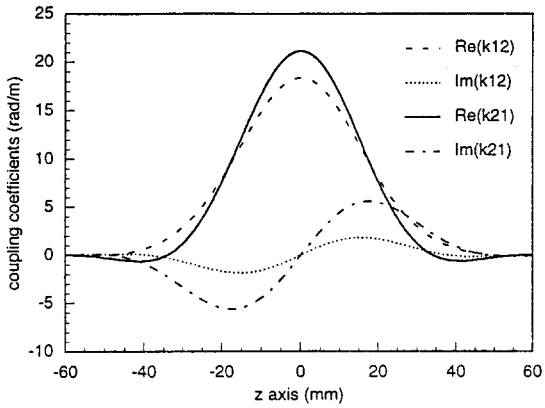

Fig. 4. The complex coupling coefficient between the disk and the straight waveguide.

$<z<+60$ mm and very little coupling occurs outside of this range. Since the amount of the coupling is less than 0.1% of maximum value (at $z=0$ mm), it is possible to neglect the coupling of outside.

In order to solve the coupled mode equation (Eq. 6) numerically, for the case that the straight waveguide is excited, we give initial values for the Eq. 6 on $z=-60$ mm;

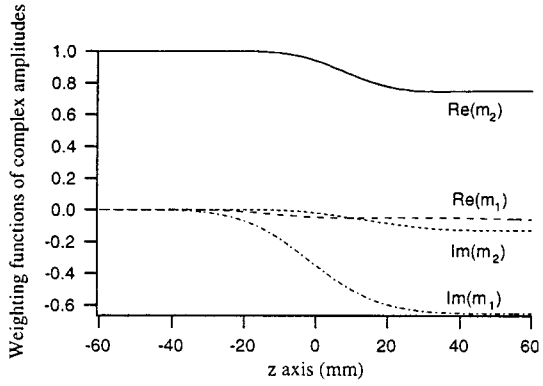

Fig. 5. The calculated results of the complex weighting functions $m_1(z)$ and $m_2(z)$ along the grobal coordinate. Initial condition is given in Eq. 8.

$$m_1(z=-60\text{ mm})=0,\quad m_2(z=-60\text{ mm})=1 \tag{8}$$

Fig. 5 shows the weighting functions $m_1(z)$ and $m_2(z)$.

A coupled field distribution is also obtained by substituting the $m_1(z)$ and $m_2(z)$ into the Eq. 1 and shown in Fig. 6.

From this figure, we can find that a part of the traveling field in the straight guide is coupled into the W. G. mode gradually. On the disk, intensity of a maximum coupled field is about -5 dB.

We also obtain transferred power from the straight guide to the disk, named here P_1 and remaining power on the straight guide, P_2. The P_1 is given in terms of the entire coupled electric field and the intrinsic magnetic field of the disk[7];

$$P_1=\frac{1}{4}\left|-\int\int_{-\infty}^{\infty}[m_1(x',\theta)e^{-j\gamma_2}E_{y'} +m_2(x',\theta)e^{-j\gamma_2}E_{y''}]H_{x'}dx'dy'\right|^2 \tag{9}$$

Resulted transferred power (P_1) is shown in Fig. 7.

In this figure, it is found that the P_1 is a function of θ and it depends strongly on the distance d.

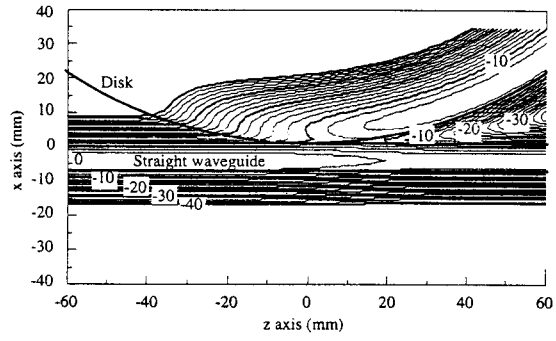

Fig. 6. The contour map of the calculated result of the coupled electric field distribution on the coupled region.

The remaining power on the straight waveguide (P_2) is also obtained in terms of the entire coupled electric field and the intrinsic magnetic field of the straight waveguide;

$$P_2=\frac{1}{4}\left|-\int\int_{-\infty}^{\infty}[m_1(z')e^{-j\gamma_1}E_y' + m_2(z')e^{-j\gamma_2}E_y']H_x'\,dx'\,dy'\right|^2 \quad (10)$$

The P_2 around the guide varies with the guide axis, and is shown in Fig. 8.

The P_2 also depends on the distance d. From this Figure, it is found that the remaining power conserves 0 dB approximately while z is less than -40 mm. It explains that no electromagnetic coupling occurs between the disk and the straight waveguide. As the results, the electromagnetic coupling occurs only in the inside of the coupled region for which we take a region from $z=-60$ mm to $z=60$ mm in this paper. It is also found that the electromagnetic coupling between the disk and the straight waveguide increases according as the distance (d) between those decreases. In the Fig. 8, it is found that the remaining power increases from $z=30$ mm, which comes from re-coupling, that is a part of the transferred power from the straight waveguide to disk returns to the disk through the electromagnetic coupling.

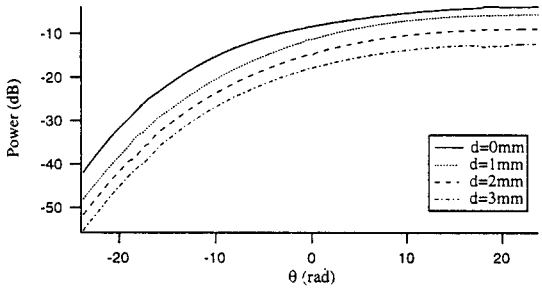

Fig. 7. Calculated results of the transferred power (P_1) from the straight waveguide to the disk.

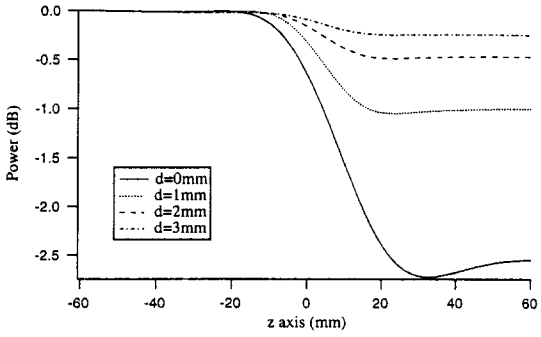

Fig. 8. Calulated results of the remaining power (P_2) on the straight waveguide.

To verify the power conservation law, we evaluate transmitting power which pass through x−y plane at $z=0$. It is found that a discrepancy between the analytical result and the law is less than 2%.

Ⅳ. Resonance characteristics of the dielectric disk with external waveguide

The coupled mode equation mentioned above is for the coupled region of a straight dielectric waveguide and a part of the dielectric disk. This part of the disk is considered as a curved dielectric waveguide. Outside of the coupled region on the disk, we consider that the W. G. mode doesn't couple to any electromagnetic field and propagates with its own propagating constant. In this case, this region is regarded as a curved waveguide where an electromagnetic mode propagates with equal propagating constant to the W. G. mode. In Fig. 9, we show an equivalent circuit of the disk resonator with external waveguide.

In this figure, we suppose that the coupled region is expressed 4-ports directional coupler, while the outside region is regarded as a transmission line. Complex amplitudes a_n and b_n show incident and reflected waves at a port n, respectively. Scattering matrices for resonator

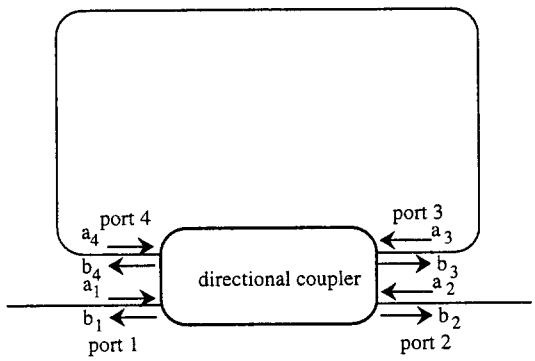

Fig. 9. The equivalent circuit of the disk resonator with the external circuit.

are given as follows[3];

$$\begin{bmatrix} b_1 \\ b_2 \\ b_3 \\ b_4 \end{bmatrix} = \begin{bmatrix} 0 & s_{12} & s_{13} & 0 \\ s_{21} & 0 & 0 & s_{24} \\ s_{31} & 0 & 0 & s_{34} \\ 0 & s_{42} & s_{43} & 0 \end{bmatrix} \begin{bmatrix} a_1 \\ a_1 \\ a_3 \\ a_4 \end{bmatrix} \tag{11}$$

$$\begin{bmatrix} a_4 \\ a_3 \end{bmatrix} = \begin{bmatrix} e^{-\phi_f} & 0 \\ 0 & e^{-\phi_b} \end{bmatrix} \cdot \begin{bmatrix} b_3 \\ b_4 \end{bmatrix} \tag{12}$$

where, $\Phi_f = \alpha_f + j\beta_f$ and $\Phi_b = \alpha_b + j\beta_b$.

Φ_f is constructed by total phase shift(β_f) and total attenuation(α_f) from port 3 to port 4 through uncoupled region. Φ_b is from port 4 to port 3 through uncoupled region. In the Eq. 11, the scattering parameter s_{ij} is given as a rate of that the complex amplitude of the port i to that of the port j;

$$s_{ij} = \frac{\left| \iint_{-\infty}^{\infty} [E_c \times H_l] \cdot \hat{\theta}\, dxdy \right|^{1/2}_{at\ port\ i}}{\left| \iint_{-\infty}^{\infty} [E_c \times H_l] \cdot \hat{z}\, dxdy \right|^{1/2}_{at\ port\ j}} \tag{13}$$

In this equation, $\boldsymbol{E}_c$ is the coupled electric field for the coupled region, and $\boldsymbol{H}_l$ is the magnetic field for the straight waveguide or for the disk. When the subscripts i and j are 1 or 2, the $\boldsymbol{H}_l$ should be taken a magnetic field of the straight waveguide mode, contrary the subscripts i and j are 3 or 4, the $\boldsymbol{H}_l$ should be taken a magnetic field of the disk(W. G. mode). When the port 1 is excited by its propagating mode, the output power from the port 2 is obtained from Eq. 11 and 12 as follows;

$$\left|\frac{b_2}{a_1}\right|^2 = \left| \frac{S_{21} - (S_{21} S_{34} - S_{24} S_{31}) e^{-\phi_f}}{1 - S_{34} e^{-\phi_f}} \right|^2 \tag{14}$$

We calculate this value on frequency range from 23.2 GHz to 23.8 GHz. Power transmission characteristic through port 1 to port 2 is obtained and shown in Fig. 10(solid line).

From this figure, it is found that the resonances occur at 23.371 GHz(mode number 57 : $WGH_{57,1,1}$), 23.703 GHz(mode number 58 : $WGH_{58,1,1}$) and the FSR(Free Spectral Range) between the two resonance frequencies is 332 MHz.

V. Experimental study for the disk resonator with external waveguide

The resonance frequencies of the disk resonator with the external waveguide on 23 GHz band have been measured experimentally on a test structure having the same dimension as

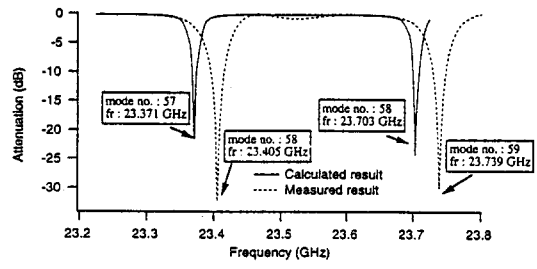

Fig. 10. Resonance characteristics of the disk resonator with external waveguide. Solid line is calculated result and dashed line is experimental one.

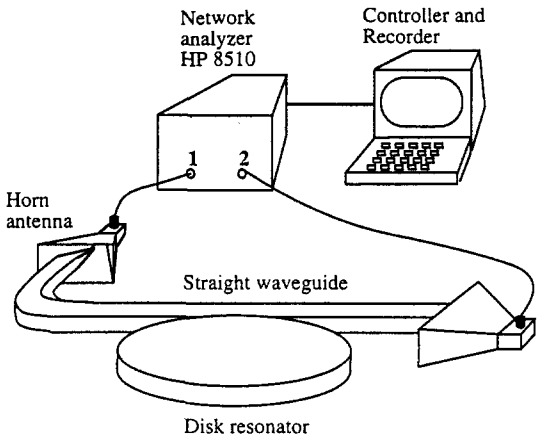

Fig. 11. The measurement setup for the resonance characteristics of the disk resonator.

the calculated ones. Fig. 11 shows the employed measurement setup.

The straight waveguide is excited by a horn antenna and the resonance characteristics are measured by HP8510. The dashed line in Fig. 10 shows the measured resonance characteristics. From these measured results, it is found that the resonances occur at 23.075 GHz(mode no. 57, the frequency range is not expressed inh this figure), 23.405 GHz (mode no. 58) and 23.739 GHz(mode no. 59). It is also found that and the FSR between mode no. 57 and 58 is 330 MHz, and between mode no. 58 and 59 is 334 MHz. As these results, it is found that the discrepancy between the theoretical and the experimental resonance frequencies is about 1.28% at mode no. 57, and about 1.27% at mode no. 58. Furthermore the discrepancy between theory and experiment of FSR(interval between mode no. 57 and 58)is about 0.6%. The discrepancies between the theories and the experiments are mainly concerned with accuracy of the propagation constant of W.G. mode referred from[6].

Furthermore, the mode numbers of the W. G. are experimentally measured to verify the theoretical results. Fig. 12 shows the measurement setup. In this figure, the x-y-z robot moves toward the θ direction on the upper plane of the disk. It also picks up amounts of phases of electric fields when the θ is increased by every 1 degree. The mode numbers are decided by the total amount of the phase shifts on circumference when it is divided by 360 degree(for example, the total amount of phase shift of mode no. 58 is 20880 degree).

Ⅵ. Conclusions

A novel analytical approach for the resonance characteristics of a disk resonator operated in a W. G. mode with an external circuit is presented. On the analysis, we divided this structure into two regions, i. e. a coupled region and an uncoupled region.

On the coupled region, the coupled mode equation based on the Lorentz reciprocity theorem is presented to analyze coupling characteristics of two nonparallel and curved dielectric waveguides. The equation is applied to the coupling between the W. G. mode in a dielectric disk and a dominant mode in a rectangular dielectric waveguide. The coupling coefficients of these two modes are numerically obtained. The field distribution around the coupling region is calculated. The transferred powers between two modes are also obtained numerically. A scattering parameter matrix for this coupled region is obtained numerically by calculating modal amplitudes of the propagating modes on the disk and the external waveguides.

On the uncoupled region, only the propagating constant of a W. G. mode is considered to the calculation of scattering parameters. The

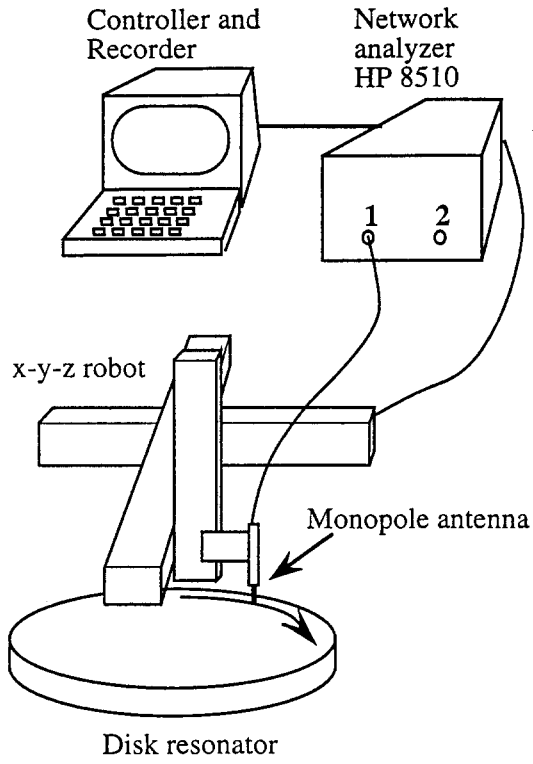

Fig. 12. The measurement setup for the mode number of the W. G. mode.

resonance frequencies are obtained numerically by solving the scattering matrix equation for these two regions. Finally, the resonance frequencies are measured on the same case. As these results, it is found that the discrepancy between the theoretical and the experimental resonance frequencies is about 1.28% and the discrepancy betwee theory and experiment of FSR is about 0.6%

The analytical method and the results of this work will be useful to precise design of high Q resonator made of dielectric on the millimeter wave integrated circuit.

References

[1] X. H. Jiao, P. Guillon, L. A. Bermudez and P. Auxemery, "Whispering-gallery modes of dielectric structures; applications to millimeter-wave bandstop filters," *IEEE Trans. Microwave Theory and Tech.*, vol. MTT-35, no. 12, pp.1169-1175, Dec. 1987.

[2] C. Vedrenne and J. Arnaud, "Whispering -gallery modes of dielectric resonator," *IEE Proc.* vol. 129, Pt H, no. 4, Aug. 1982.

[3] M. Muraguchi, K. Araki and Y. Naito, "A new type of isolator for millimeter-wave integrated circuits using a nonreciprocal traveling-wave resonator", *IEEE Trans. Microwave Theory and Tech.*, vol. 30, no. 11, pp.1867-1873, Nov. 1982.

[4] H. A. Haus, W. P Huang and A. W. Snyder, "Coupled-mode formulations," *Optics Letters*, vol. 14, no. 21, pp. 1222-1224, Nov. 1989.

[5] S. Chuang, "A coupled mode formulation by reciprocity and a variational principle," *IEEE J. Lightwave Tech.*, LT-5,1, pp. 5-15, Jan. 1987.

[6] Y. Tomabechi and K. Matsumura, "Resonance characteristics of whispering gallery mode on a dielectric disk," *IEICE Trans.* C-I, vol. J75-C-I, pp.687-693 Nov. 1992.

[7] A. Hardy and W. Streifer, "coupled mode theory of parallel waveguides," *IEEE J. Lightwave Tech.*, LT-3,5, pp.1135-1146, Oct. 1985.

황 재 효

1990년 2월 : 아주대학교 전자공학과 (공학사)
1992년 8월 : 광운대학교 대학원 전자공학과(공학석사)
1996년 9월 : 일본 우츠노미야대학 대학원 생산정보공학전공 (공학박사)
1996년 3월~현재 : 영동대학교 전자공학부 조교수
[주 관심분야] 전파전파 및 초고주파 회로

민 경 일

1977년 2월 : 울산대학교 전자공학과
1984년 8월 : 충남대학교 대학원 전자공학과(공학석사)
1995년 2월 : 충남대학교 대학원 전자공학과(공학박사)
1996년 3월~현재 : 영동대학교 전자공학부 조교수
[주 관심분야] 안테나 및 초고주파 회로

구 경 완

1983년 2월 : 충남대학교 전자공학과 (공학사)
1985년 2월 : 충남대학교 대학원 전자공학과(공학석사)
1992년 2월 : 충남대학교 대학원 전자공학과(공학박사)
1989년 3월~1994년 2월 : 충청전문대학 전자과 조교수
1994년 3월~현재 : 영동대학교 전자공학부 부교수
[주 관심분야] 광 집적화 소자 및 초고주파 소자